

# Estimation of near-surface attenuation in the tectonically complex contact area of the Northwestern External Dinarides and the Adriatic foreland

Snježana Markušić<sup>1</sup>, Davor Stanko<sup>2</sup>, Tvrko Korbar<sup>3</sup>, Ivica Sović<sup>1</sup>

5 <sup>1</sup>University of Zagreb, Faculty of Science, Zagreb, Croatia

<sup>2</sup>University of Zagreb, Faculty of Geotechnical Engineering, Varaždin, Croatia

<sup>3</sup>Croatian Geological Survey, Zagreb, Croatia

*Correspondence to:* Snježana Markušić (markusic@irb.hr)

**Abstract.** Seismic-induced ground motion at a site is generally influenced by the seismic source, the propagation path and the local site conditions. Over the last several decades, researchers have consistently asserted that for near site attenuation, the spectral parameter kappa is subject primarily to the site conditions. In this research we estimated the parameter kappa, based on the acceleration amplitude spectrum of shear waves, from local earthquakes recorded by seismological stations situated in the western part of Croatia from the slope of the high-frequency part. The spatial distribution of kappa values is comparable with seismological, geophysical and geological features, with the published coda- $Q$  values for each station as well as with the isoseismal maps for selected stronger earthquakes in the study area. The complex pattern of longitudinal and transversal major late-orogenic fault zones dissecting early-orogenic thin-skinned tectonic cover in the Kvarner area, and the shallow depth to the Moho in the Adriatic foreland (southern Istria) are probably responsible for significant part of wave attenuation and for the anisotropy of attenuation. Regional near-surface attenuation distribution and modelled macroseismic fields point to conclusion that attenuation properties of rocks in the Northwestern External Dinarides are far from isotropic and the most likely anisotropy sources are the preferential orientations of cracks and fractures under the local tectonic stress field, trapping of waves along major faults (waveguides), and/or attenuation within the fault zones. These results are important for gaining further insight into the attenuation of near-surface crust layers in the Northwestern External Dinarides and the associated Adriatic foreland, as well as in similar geotectonic settings.

25 **Keywords:** Northwestern External Dinarides; near-surface attenuation; spectral parameter kappa;  $V_{s30}$  value; coda- $Q$  value; isoseismal map.

## 1 Introduction

It is a well-known fact that earthquake shaking at the particular site in terms of observed or recorded strong ground motion is subject to complex source characteristics, attenuation of seismic waves when they propagate through the Earth's crust, and changes resulting from local site conditions (e.g., Reiter, 1990).

5 Attenuation of seismic waves is a key factor in seismic hazard assessment for earthquake prone regions. It is also important for quantification of earthquakes and plays a significant role in studies of seismic source or crustal structure.

This paper presents the calculated values of the high-frequency parameter  $\kappa$  (Anderson and Hough, 1984) and the local site-specific component  $\kappa_0$  (also called near-site or near-surface attenuation) in the area of Northwestern External Dinarides and the respective Adriatic foreland, based on recordings from four Croatian seismological stations. The area under research is

10 shown in Figures 1 and 2 and covers the region of Istria and part of the northern Adriatic offshore area (the Adriatic foreland), as well as the Kvarner islands, wider area of Rijeka, the northern Dalmatian islands, and the regions of Lika and Gorski kotar (the Northwestern External Dinarides).

The major contribution to the seismic energy dissipation at sites and to the high-frequency part of the Fourier-amplitude spectrum (*FAS*) of S-waves (for which the near-site attenuation parameter  $\kappa_0$  describes rapid decay) comes from top surface 15 layers till depths of 1–2 km (comprising sedimentary soils and rocks and especially for close distances, less than 50 km).

The high-frequency attenuation parameter  $\kappa$  is calculated from the slope of the *FAS* in the linear–logarithmic space for the high-frequency range of the S-wave window. Calculated individual horizontal  $\kappa$  values for EW and NS components were combined to provide an average value of  $\kappa_{hor}$  for each earthquake event. Using the Anderson and Hough (1984) approach, individual  $\kappa$  values are paired with epicentral distances  $R_e$ . For all analysed stations a gradual increase of  $\kappa$  with epicentral 20 distance  $R_e$  is observed.

Therefore, the  $\kappa - R_e$  model is used to estimate the value of the site-specific (near-site) attenuation parameter as a zero-distance  $\kappa_0$  value. Over the last three decades, the near-site attenuation parameter  $\kappa_0$  has been regularly used in various 25 applications, particularly in devising and calibrating ground-motion prediction equations (GMPEs) which are based on stochastic simulations (e.g., Hanks and McGuire, 1981; Boore, 1983; 2003; Ktenidou et al., 2014), host-to-target adjustments of GMPEs (e.g., Campbell, 2003; Biro and Renault, 2012; Delavaud et al., 2012) and site-specific ground response analysis for critical facilities. For  $\kappa_0$ , the term near-site attenuation is used, given that it ‘captures’ attenuation effects near and below the site, i.e., within a radius of few kilometres around the site.

To address the effect of the uncertainty in  $R_e$  on the  $\kappa$ , instead of using the traditional linear least-squares regression, the linear regression suitable for data with errors, following the method by York et al. (2004), was performed.

30 Estimated regional and local variations of the spectral parameter  $\kappa$  were compared with the geological characteristics of the investigated area and with macroseismic fields for selected earthquakes.

## 2 Geological features and seismic activity

The territory of Croatia is situated on the broad Africa-Eurasian (central-northern Mediterranean) collision zone (Battaglia et al., 2004 and references therein). The Adriatic microplate (Adria) is situated in between the Nubia (Africa), Eurasian and Anatolian plates, and probably moves as an independent microplate (Battaglia et al., 2004). The Adria dips to the northeast

5 (NE) beneath the External Dinarides (Šumanovac et al., 2017), which could be considered as the detached and backthrust pre-orogenic upper sedimentary cover of the Adriatic microplate, deformed into a classical fold-and-thrust belt during the Alpine orogeny in the region (Schmid et al., 2008). The tectonic structure of the northeastern Adriatic region is subdivided into the Adriatic foreland and the External Dinarides which are crustal mega-units developed atop the subducted Adriatic microplate during the Cenozoic (Korbar, 2009). The External Dinarides are characterized predominantly by the NW-SE 10 striking faults along the eastern part of the Adriatic coast that is predominantly composed of Mesozoic shallow-marine carbonate platform formations (Vlahović et al., 2005). Though parts of the northwestern and southeastern External Dinarides are characterized by obvious thin-skinned tectonics, resulting from strong tangential movements during the main phase of the Alpine (Dinaridic) orogeny (Schmid et al., 2008 and references therein), this tectonic feature is not that obvious in the 15 investigated area of the External Dinarides (Korbar, 2009).

15 Earthquake hypocenters are distributed along the External Dinarides until a depth of 30 km (Prelogović et al., 1982; Kuk et al., 2000) and probably originate from recent tectonic activity along the complex transpressional zone striking NW-SE, causing active uplift of the main crest of the External Dinarides (Korbar, 2009 and references therein). In addition to the tangential tectonic movements, responsible for significant deformations of the affected sedimentary cover, the neotectonic phase is characterized by a horizontal shearing of neighboring tectonic units or blocks, especially along the re-activated NW-SE 20 Dinaridic faults, as well as along inferred transversal faults that have yet to be clearly described and investigated.

Upper crustal geological structures are the result of tectonic movements in the deeper parts of the lithosphere which in turn feature deformations of the supposed basement of sediments and Mohorovičić discontinuity, provided by gravimetric and seismic data (Aljinović and Blašković, 1981; Aljinović et al., 1984; Šumanovac et al., 2009; Šumanovac, 2010), that are the deep seismic data from the area recorded during the 1960s, 1970s, and within the ALPASS-DIPS projects (ALP 2002, 25 Šumanovac et al., 2009). The data imply a very coherent seismic reflector that is interpreted as „strong lithological changes occurring between Triassic carbonates and the underlying clastics” (Aljinović and Blašković, 1981) or the “Base Carbonate” reflector (BC cf. Grandić et al., 2002). The seismic data indicate that the basement of sediments in Istria and on the island of Krk has not been determined (Aljinović et al., 1984), however, with a remark that in Istria a reduced thickness of carbonate rock succession exists (Durasek et al., 1981).

30 The BC is upthrown north of the northeastern Adriatic fault zone striking NW-SE generally along the mainland coast (Korbar, 2009), and crops out in the central part of Gorski kotar (HGI, 2009). Besides, the displacement of the BC is achieved along a transversal fault striking NE-SW at the eastern boundary of the Kvarner fault zone (Aljinović and Blašković, 1981).

Nevertheless, regional geomorphology and detected tectonic lines generally correspond to the supposed and still tentatively defined Kvarner fault zone (Grandić et al., 2002; Finetti, 2005; Korbar, 2009).

The gravity map of Bouguer anomalies (Gravity map of Yugoslavia, 1972) exhibits a high coincidence with the spatial depth variation of the Mohorovičić discontinuity (e.g., Brückl et al., 2007; Orešković et al., 2011). Two facts are evident – the area

5 of positive anomalies extending NW to SE with maxima in Istria and the stretch of negative anomalies following the axis along the deepest parts of the Mohorovičić discontinuity. Furthermore, the large zone of positive magnetic anomalies in Istria is evident, but is not noticeable in either the gravity or Mohorovičić subsurface maps. The total intensity anomalies (Brdarević and Oluić, 1979) of the geomagnetic field indicate that only the deeper parts of the Northern Adriatic are slightly magnetic. The crystalline basement of sedimentary rocks is supposed to be composed of low-magnetic rocks from which the magnetic  
10 igneous rocks protruded during the geological evolution.

Local seismicity features are important since beside local and regional attenuation as primary contributions to  $\kappa$ , orientation of the earthquake epicentres can have effect on the  $\kappa$  distribution. The investigated region is moderately seismically active (Figure 1). Seismic activity in the greater Rijeka area is known for frequent occurrences of relatively weak earthquakes ( $M_L < 4.0$ ) and occasional occurrences of moderate or large ones (Ivančić et al., 2006, 2018). The earthquake foci lie at depths of up to 20 km,

15 with the seismogenic tectonic zone striking in a NW-SE direction along the coastline. It is dominated by the Ilirska Bistrica - Rijeka - Senj obliquely reverse fault system, indicating compression of the Dinarides and an oblique subduction of the Adriatic microplate (Kuk et al., 2000). Figure 3 depicts fault plane solutions of all earthquakes in Croatian source mechanism database (Archive of the Department of Geophysics) for the study area and event magnitudes  $M_w \geq 3.0$ . Displayed are so called beach-balls (stereographic projection of the lower focal hemisphere). The figure shows predominant source mechanisms with  
20 right-lateral displacement, although a lot of events indicate pure reverse faulting.

### 3 Estimation of kappa parameter and connection to quality factor Q

The Croatian WM seismological stations included in this study are: Brijuni-BRJN, Rijeka-RIY, Novalja-NVLJ and Ozalj-OZLJ, as shown by the red triangles in Figure 2. The seismograms of earthquakes recorded at the stations in the period 2002–2017 with  $M_L \geq 3.0, R_e \leq 150$  km and at focal depths of  $h < 30$  km were collected. The locations of the earthquakes are  
25 shown in Figure 2. The selection of the local magnitude and epicentral distance limit values plays a major role in calculating  $\kappa$  (Anderson and Hough, 1984; Drouet et al., 2010; Ktenidou et al., 2013). The magnitude limit and epicentral distance limit were applied to the selected recordings ( $M_L \geq 3.0, R_e \leq 150$  km) in order to exclude possible source contribution to  $\kappa$ .

The azimuthal distribution of the used data sets was limited at each station due to the nature of earthquake locations and operative years of each station, as presented in Figure 4 and Table 1.

30 As can be seen in Figure 4 most of the earthquake recordings are in the magnitude range  $3.0 \leq M_L \leq 4.0$  with the earthquake locations distributed within  $40 \leq R_e \leq 100$  km. Station NVLJ recorded more than one hundred earthquakes in the most seismically active parts of Croatia, RIY recorded 60 earthquakes in moderate seismic areas while BRJN (data only till the end

of 2013) and OZLJ recorded around 30–35 earthquakes (Table 1). As mentioned before, the number of recordings at each station depends not only on local seismicity but also on the operational period of each station.

The acceleration recordings were filtered using a band-pass filter at 0.5–25 Hz in order to exclude low frequency noise. The dropout of the *FAS* at frequencies greater than 24 Hz was due to the anti-alias filter and did not affect the estimation of  $\kappa$  from the slope of the high-frequency part of the *FAS*. The S-wave window with a minimum duration of 3 s (in some cases with part of coda waves which cannot be avoided) was selected for each record and processed using the Fast Fourier Transform to obtain the *FAS* of the S-waves. In the preliminary spectrum processing, we follow Signal-to-Noise-Ratio criteria ( $SNR > 3$ ), as recommended by Ktenidou et al. (2013). Also, it was avoided to use *FAS* of recordings that strongly deviates from exponential decay; i.e., spectrum that increases in amplitude at higher frequencies due to combined effect of the site amplification between surface and deep bedrock and path-independent zero attenuation effects (Boore and Joyner, 1997), or spectrum with presence of strong resonance effects that corresponds to site fundamental and first higher harmonics (Ktenidou et al., 2013). The Horizontal-to-Vertical Spectral Ratio (HVSR) curves recorded at the seismological stations were used as an indicator of possible strong resonance peaks at local sites which may have had an impact on estimating  $\kappa$  from the *FAS*. The HVSR methodology proposed by Nakamura (1989) has been used in numerous studies to estimate local seismic ground response as expressed by natural/fundamental frequency ( $f_{res}$ ) of soils and HVSR spectral peak amplification, particularly in the broader study area, e.g., in Slovenia (Gosar, 2007; Gosar and Martinec, 2009; Gosar et al., 2010), in Italy (Mucciarelli and Gallipoli, 2001; Di Giacomo et al., 2005; Del Monaco et al., 2013; Panzera et al., 2013), and in Croatia (Herak et al., 2010; Herak, 2011; Stanko et al., 2016, 2017).

Geological and tectonic characteristics around each station (in the vicinity of approx. 30 km) are important when defining primary factors affecting the  $\kappa$  distribution. For that purpose, local and regional geological and tectonic characteristics are analyzed and discussed based on the Explanatory notes for the Geological Map of the Republic of Croatia (Velić and Vlahović, 2009) and the cited papers. It should be noted that all the stations are situated on the hard bedrock without any superficial deposits or significant soil.

The Brijuni seismological station (**BRJN**) is situated on the island Veliki Brijuni (at an altitude of 22 m) within the Brijuni National Park, i.e., on the west coast of the Istrian Peninsula. The wider area is characterized by a slightly deformed 2000-meter thick low-fractured succession of Jurassic to Upper Cretaceous shallow-water carbonates deposited on top of the Adriatic carbonate platform (Vlahović et al., 2005). The tectonic structure of the area around the station is very simple and belongs to the Adriatic foreland (Korbar, 2009). The carbonate strata are gently inclined to the southeast in the southeast limb of wide regional foreland anticline characterized by the axis striking SW-NE along central Istria.

The wider area around the seismological station Rijeka (**RIY**) is mainly composed by strongly deformed and fractured Upper Cretaceous to Paleogene carbonates. The deformation is probably related to a thin-skinned tectonics (Korbar, 2009). Eocene flysch clastics are situated in the long synclines compressed between huge carbonate anticlines. The RIY station (at an altitude of 70 m) is situated in Rijeka City on Lower Cretaceous deposits consisting of limestones and dolomites that are approx. 500–600 m thick. The overall thickness of the thin-skinned sedimentary cover cannot easily be estimated due to the lack of

boreholes as well as due to a complex tectonic structure in the area. However, in the deep borehole located in the central part of the neighboring island of Krk, carbonates are more than 3500 m thick, while the supposed thin-skinned, highly fractured part is at least 1500 m thick (Korbar, 2009).

The wider area of the Novalja seismological station (**NVLJ**), situated on the Pag Island, consists of intensely fractured Upper Cretaceous to Paleogene carbonates in long anticlines which in the crestal parts consist of limestone breccia deposited in the axial zones. Flysch clastics are situated in the synclines, similarly to those in the Rijeka area, given that both areas belong to the thin-skinned sedimentary cover. The NVLJ seismological station (altitude 10 m) is situated in Novalja on the Pag Island within the area mainly composed of limestone breccia of unknown thickness, while the modelled thin-skinned carbonates are up to a few thousand meters thick (Korbar, 2009).

The Ozalj station (**OZLJ**) is situated in the transition zone between the Dinarides and the Pannonian Basin, in a zone consisting mainly of deep-water carbonates and clastics that are covered by thin alluvium along the Kupa river valley. The wider area of the Ozalj seismological station (OZLJ) paleogeographically belongs to a carbonate platform-to-basin transition, which is in its recent structural position tectonically roughly equal to a front of a major overthrust with a southwestern vergence. The station itself is situated on the cliff hillside of the Kupa River (at an altitude of 186 m) and is composed of deformed Upper Cretaceous flysch succession that is approx. 400–500 m thick, and transgressively overlies the strongly fractured older carbonates.

In order to estimate the value of the site-specific (near-site) attenuation parameter  $\kappa_0$ ,  $\kappa$  models as a function of epicentral distance are proposed using the Anderson and Hough (1984) approach. Instead of using traditional linear least-square regression, linear regression for data containing errors and following the method by York et al. (2004) was applied to identify possible correlation for observational errors in two coordinates ( $R_e$  and  $\kappa$ ). Typically, the standard error for  $R_e$  amounts to  $\pm 3$ –5 km (Marijan Herak, personal communication) and for these particular cases, with error in  $\kappa$  set to 2 standard deviations ( $\sim 0.01$ –0.02 s), differences between standard linear regression and error-in-variables linear regression are less than 5 %. With less data, large data scatter and lack of data at shorter epicentral distances, differences between two regression methods could be significant. Therefore, for shorter epicentral distances we set errors to be in order of 5 km, while for higher distances ( $> 100$  km) we set it to 10 km. The summarized results of errors-in-variables regressions (following the method by York et al., 2004) for the  $\kappa - R_e$  dependence based on horizontal and vertical  $\kappa$  models ( $\kappa_{hor}$  and  $\kappa_{ver}$ ) using the AH84 (Anderson and Hough, 1984) approach are shown in Figure 5 and given in Table 2 with estimated site-specific attenuation values of  $\kappa_0^{hor}$  and  $\kappa_0^{ver}$  and regression slopes  $\kappa_R^{hor}$  and  $\kappa_R^{ver}$  for each seismological station.

The slopes of regression lines,  $\kappa_R$ , (Figure 5 and Table 2) indicate a gradual increase of  $\kappa$  with the epicentral distance  $R_e$  for all stations, consistent with the findings of Anderson and Hough (1984) and Ktenidou et al. (2013, 2015). The large scatter of data points is typical in  $\kappa$  studies as reported in the cited literature. Nearby recordings can constrain the site-specific  $\kappa_0$  and distant recordings can constrain propagation path effects through the slope of regression  $\kappa_R$ . Numerous researchers studying kappa have reported that a gradual increase may begin at distances of 15–20 km, hence implying a regional attenuation effect in the Earth's crust, whereas the mean  $\kappa$  values are somewhat constant (similar to the site-specific  $\kappa_0$ ) at short distances. This

effect seems to be true mainly due to limited data for shorter epicentral distances. The main attenuation contribution in  $\kappa_0$  is due to the local site effects of the shallow crust near and below the site (up to depths of 1–2 km), as reported by Van Houtte et al. (2014) and Ktenidou et al. (2015). This is the reason why kappa-researchers use several terms (near-site attenuation, site-specific attenuation, or simply site attenuation) to describe the  $\kappa_0$  parameter at zero-distance or at short epicentral distances.

5 The values of site parameter  $V_{S30}$  (average shear wave velocity in the top 30 m of soil) that is correlated with local geological characteristics of each station, can be compared to the estimated site-specific attenuation  $\kappa_0$  values, and based on Tables 1 and 2, indicates that these two values are inversely proportional (Ktenidou et al., 2014).

Figure 6 shows a spatial regional  $\kappa$  variation in the investigated area around each station (individual  $\kappa$  values are plotted using the nearest-neighbour interpolation method). Different trends of high-frequency attenuation between north-eastern and south-

10 western azimuthal area subsets can be observed. Based on the observations, one possible explanation is that the weaker or higher attenuation expressed in the regional  $\kappa$  variations results from a large dispersion in individual  $\kappa$  estimates at the near-fault zones and is related to S-wave reflections. The spatial  $\kappa$  distribution presented in Figure 6, shows that attenuation properties of rocks in the Northwestern External Dinarides are far from isotropic. The source of this anisotropy is still not confidently determined – the most likely candidates are the preferential orientations of cracks and fractures under the local 15 tectonic stress field, trapping of waves along major faults (waveguides), or attenuation within the fault zones which is discussed in more details in the next chapter.

It is possible that large regional discrepancies in the values of  $\kappa_0$  exist for similar sites due to regional differences of the underlying crustal  $Q$  and  $V_s$  profile for similar  $V_{S30}$  values (e.g., Boore and Joyner, 1997; Chandler et al., 2006). The conclusions should be drawn with caution due to the limited number of data at shorter distances and the narrow azimuthal 20 datasets (Figure 4). This is a major limitation when using Anderson and Hough's (1984) classical  $\kappa$  approach to areas of low-to-moderate seismicity and is due to the limited quantity and bandwidth of usable data. Even if the trend of  $\kappa$  with distance is clearly visible for all cases, more data that will be collected in the future may provide more evidence and resolution for the shortest distances, especially for stations where the lack of data is most prominent.

The high-frequency spectral attenuation parameter  $\kappa$  was calculated from the acceleration *FAS* of the S-waves under the 25 assumption that the effective quality factor  $Q$  in near-surface rocks (at approx. depths of up to 2–3 km) is frequency-independent. In this case, the frequency-independent effective quality factor  $Q_{est}$  at high frequencies can be estimated from the regression slope of the empirical model,  $\kappa_R$  (e.g., Anderson and Hough, 1984; Edwards et al., 2011; Gentili and Franceschina, 2011; Ktenidou et al., 2015):

$$Q_{est}(\kappa_R) \approx \frac{1}{\beta_0 \kappa_R}$$

30 where the average crustal shear wave velocity was assumed to be  $\beta_0 = 3.5$  km/s. The ratio of the slopes  $\kappa_R$  for horizontal and vertical components are similar, i.e., approx. 1 (see Table 2). Therefore, only the horizontal value of kappa is used for the spatial kappa distribution and estimated  $Q$  values,  $Q_{est}(\kappa_R)$ , when describing regional attenuation.

Several studies indicated possibility that  $Q_{est}^{C,S}(f)$  from the coda waves (or S-waves) estimated for the high-frequency range and  $Q_{est}(\kappa_R)$  calculated from  $\kappa_R$  yield approximately similar values (e.g., Edwards et al., 2011; Gentili and Franceschina, 2011; Ktenidou et al., 2013, 2015). Table 3 compares the estimated values of frequency-dependent  $Q_{est}^C$  (for the high-frequency range, 10–25 Hz) from recent attenuation studies of coda waves in Croatia (Dasović et al., 2012, 2013; Dasović, 2015) with the frequency-independent  $Q_{est}(\kappa_R)$  from this study. Taking into account inherent errors of  $Q$  and  $\kappa$  measurements, the corresponding values for the Croatian station given in Table 3 show that this is mostly also the case here. This comparison helps to verify the accuracy of the regression slope  $\kappa_R$  from the  $\kappa - R_e$  models, but it also includes certain complexities (e.g., different data ranges for magnitudes and epicentral distances, the impact of frequency-dependent scattering attenuation and frequency-independent intrinsic attenuation having an effect on the  $\kappa$  value). Taking into consideration the issues 5 enumerated above, the results presented in Table 3, as well as similar conclusions of other studies, hint to the conclusion that the high-frequency decay of  $FAS$  as modelled by  $\kappa$ , has its roots in anelastic (intrinsic) and scattering attenuation properties of the rocks along the path from the source to the receiver. Moreover, it may be possible that similar sites exhibit significantly 10 large regional differences due to the variability of the underlying  $Q$  and  $V_S$  structures (e.g., Boore and Joyner, 1997; Chandler et al., 2005; Ktenidou et al., 2014). Keeping all this in mind,  $Q$  values calculated from coda waves and kappa values (Table 3) 15 are considered comparable, while taking into account inherent errors of  $Q$ - and  $\kappa$ -measurements (often of the order of  $\pm 50\%$ ).

The values of  $Q_{est}(\kappa_R)$  (Table 3) that actually represent the total average regional crustal attenuation in the vicinity of each station, may be linked to major tectonic units. Hence, the value of  $Q_{est}(\kappa_R)$  for the OZLJ station may represent a transitional 20 zone between the Pannonian Basin and the Internal Dinarides (e.g., Tomljenović et al., 2008). In addition, the values of  $Q_{est}(\kappa_R)$  may define the transition zone from the undeformed Adriatic Microplate (the BRJN station) into the deformed part of the Dinarides (the RIY and NVLJ stations) (e.g., Handy et al., 2015). The value given in Table 3 for the BRJN station is comparable 25 to the average value determined for crustal depths varying from 5 to 15 km and which were published by Gentili and Franceschina (2011) for the area of the southeastern Alps and northern External Dinarides in Northeastern Italy (Friuli-Venezia-Giulia).

#### 25 **4 Discussion of the parameter kappa within regional seismological and geological characteristics**

The attenuation is possibly related to a highly fractured thin-skinned tectonic cover in the hanging-wall of the frontal Dinaridic thrust that differs from the less fractured carbonates below the major detachments, as well as from the less fractured carbonates in the Adriatic foreland. It must be noted, that the uppermost detachment horizon (major thrust faults) appears on the surface 30 along the demarcation line between Gorski Kotar and the Kvarner area. The horizon is irregularly distributed within the investigated region due to the late-orogenic exhumation of the Dinarides and still insufficiently defined regional dextral shift of the frontal thrust of the External Dinarides along the Kvarner fault zone (Grandić et al., 2002; Korbar, 2009; Aljinović and

Blašković, 1981). The dextral shift along the Kvarner fault zone was also detected on deep seismic images on the crustal scale (Finetti, 2005).

Weaker attenuation properties (see Fig. 6) may also be caused by S-wave reflection from different parts of the shallower Mohorovičić discontinuity (see Fig. 7), at a depth of about 25–30 km (e.g., Gentili and Franceschina, 2011). This is exactly the case for the Adriatic foreland part along the southwestern coast of Istria, where the Mohorovičić discontinuity depths vary from about 27 km (Finetti, 2005) to approx. 40 km (Brückl et al., 2007; Grad et al., 2009). These effects can be explained by observations that fault zones are often characterized by complex rupture pattern that favour both scattering and generation of trapped waves (within the waveguides) in terms of 10–20 km propagation through low velocity and spatial variation of low intrinsic  $Q_i$  near the source, caused by the high level of fracturing that characterizes the fault zones.

Several authors have analyzed attenuation in tectonized (fractured) and non-tectonized carbonates. Johnston et al. (1979) proposed numerous mechanisms to explain attenuation (of seismic waves) in rock masses. One of the listed mechanisms, according to Barton (2007), can be extended to major discontinuities, rock boundaries and faults in tectonic fractured and/or stressed rock masses. Barton strongly supports the idea that seismic  $Q$  values provide good insight into rock mass characteristic – where low  $Q$  values correspond to poorer, more jointed, more open structures, typical of near surface rocks. Abercrombie (1998) determined that joints and fractures acted as major scatterers of seismic energy. The possible reasons for strong attenuation at a shallow depth can be attributed to high fracture densities at outcrops and the presence of joints at moderate or low pressures. A reduction of seismic attenuation with respect to depth is expected due to a reduction of the number of joints/fractures and greater closure with higher stress. Worthington and Hudson (2000) investigate whether any useful information about a fault can be obtained from attenuation and concluded that relatively high values of attenuation were found in the fault zone. They identified the  $Q$  anomaly as a result of certain changes in rock properties.

Belinić et al (2018) indicated the presence of a boundary area between the thicker lithosphere under the Northwestern External Dinarides and the thinned lithosphere under the Lika region, that is recognized by Šumanovac et al (2017) as the ND-anomaly (North Dinaridic fast velocity anomaly, discovered by the teleseismic tomography). Interestingly, the ND-anomaly in the area of Gorski kotar (e.g., Šumanovac and Dudjak, 2016; Šumanovac et al., 2017) partly fit the observed kappa decrease. It could be speculated that the North Dinaric fast velocity anomaly (ND-anomaly), identified on the teleseismic tomography for the wider Kvarner, may be related to the lithospheric transform zone striking transversally to the Dinarides below the Kvarner area (Korbar, 2009), possibly delineating the boundary between the NW and SE Adriatic microplate fragments recognized by Oldow et al. (2002). If that is the case, the differential movements of the two Adria fragments is accommodating along crustal faults that evidently have not fully dissected the thin-skinned tectonic cover, given that there is more or less continuous but bent fold-and-thrust belt in the NW part of the External Dinarides (Placer et al., 2010).

## 5 Macroseismic field

Spatial distribution of macroseismic intensities is generally influenced by major geological and tectonic features (Bottari et al., 1984) and, on a smaller scale, by local geological conditions, such as the surface soil, the surface-to bedrock soil structure in sedimentary basins and the depth of the saturated zone (Seed and Schnabel, 1972). Also, the distribution of macroseismic 5 intensities may reveals the large tectonic features (Besana et al., 1997; Bottari et al., 1984; Hashida et al., 1988; Lekkas, 2001). Study of the macroseismic field can give information about near-surface attenuation of the seismic waves in frequency range of 0.4-13 Hz (Sokolov, 2002).

In this paper, are displayed macroseismic fields for the chosen set of six earthquakes (Table 4) with epicenters located in the study area. Earthquakes occurred in the period 1870 – 2013, and for majority of them macroseismic intensities are more reliable 10 source of information than instrumental data. Magnitude range of chosen events is 4.7 – 5.8. The strongest earthquake on March 12, 1916 near Grižane. It was very strong event with maximum intensity  $I_{max}$  = VIII MSK.

Macroseismic fields (the synthetic isoseismals) are modelled using the SAF (Strong Attenuation at Faults zones) model (Sović and Šariri, 2016) (Figure 8). This model assumes that the active faults attenuate macroseismic intensities, hence the most 15 important input data is a map of the active faults. For that purpose, the information on faults were taken from the Map of Active Faults in Croatia (Ivančić et al., 2006). The synthetic isoseismals (Figure 8) are compared with the empirical ones by using moment analysis method (Sović et al, 2013; 2016; Sović and Šariri, 2018). The results show that synthetic isoseismals are 1.4% better approximation of empirical macroseismic field (Sović and Šariri, 2018) than classical model (Kövesligethy, 1907). From these results it is evident that fault zones are responsible for significant part of wave attenuation 20 and for the anisotropy of attenuation. Synthetic isoseismals are similar but not identical to the empirical ones because the wave attenuation at fault zones is only one of the mechanisms which modify macroseismic field. The shape of macroseismic field also depends on the other factors like amplification of the shallow sedimentary layers (Seed et al., 1972), topography (Geli et al., 1988; Buech et al., 2010) and deamplification due to nonlinear effects (Beresnev and Wen, 1996). Intensity amplification by site effects can be seen on the Figure 8 (cases b-f), where empirical intensities in deep soil zones NE from central areas (river valleys in Gorski Kotar, Slovenia and Pannonian basin) are greater than synthetic ones. Similarity of synthetic and 25 empirical isoseismals in areas with negligible site effects means that the strong attenuation of macroseismic intensity at fault zones is a assumption.

Attenuation of macroseismic intensity is consequence of attenuation of seismic waves caused by high level of fracturing in fault zones (Gentili and Franceschina, 2011), and temporary decrease of shear modulus in fault core under the influence of incoming waves (Johnson and Jia, 2005), thus, the attenuation of macroseismic field can be linked to the parameter kappa by 30 the same physical mechanisms.

## 6 Estimation of near-surface attenuation – summary and conclusions

The main problem associated with the regional  $\kappa$  variation/attenuation and its connection with the geological and tectonic environment at a local and regional level is in a proper definition of the tectonics (deformed or undeformed plates, fault description) and the thickness of the shallow crustal deposits with different geological characteristics at each station's area.

5 As suggested by Gentili and Franceschina (2011), higher  $\kappa$  values can be linked to a high level of fracturing (that characterizes fault zones). The major contribution to the total  $\kappa_0$  is due to the sedimentary column (from the surface level to a depth of 800 m). Furthermore, Campbell (2003) recognized that the scattering effects, due to small-scale heterogeneities in the geological profile beneath the recording stations, may have a significant impact on the final  $\kappa$  values.

Based on the calculated kappa values, the published  $Q$  values, empirical and modelled macroseismic fields and geological

10 features of the area of the Northwestern External Dinarides and the associated part of the Adriatic foreland, the following can be concluded:

- In the coastal area (Velebit area) near-surface attenuation is lower in the NW-SE direction. To the west, the reduction of attenuation becomes more pronounced in the SW-NE direction (area of the Krk Island), hence in the southern part of Istria the lower attenuation is more dominant in a SW-NE direction;
- Given that the modelled macroseismic fields are well matched with empirical data, and also based on observations of near-surface attenuation as defined based on the kappa parameter, the modeling performed in this paper is applicable when assessing local near-surface attenuation (in the investigated area) under the assumption of a realistic earthquake scenario;
- Regional geological variability is important for estimating near site attenuation  $\kappa_0$ ;
- The values of  $V_{s30}$  can only be compared with the estimated  $\kappa_0$  values and, based on Tables 1 and 2, the conclusion is that these two values are inversely proportional;
- $Q$  values calculated from coda waves and those estimated from kappa values (Table 3) are considered to be comparable (subject to certain limitations);
- There is an indistinct correlation between the observed attenuation and the rate of tectonic deformation of the platform carbonates in the fold-and-thrust belt (more deformed and more fractured) and in the foreland (less deformed and less fractured);
- It may be hypothesized that the observed lower attenuation west of the southwestern coast of Istria is caused by S-wave reflection from parts of the Mohorovičić discontinuity at depths below 30 km;
- When taking all this into consideration, the dextral shift of the frontal thrust from the External Dinarides along the Kvarner fault zone and the deeper position of the “Base Carbonate” (BC) horizon east of the zone, has probably had an effect on the geometry of the kappa parameter contour lines, i.e., observed attenuation in the investigated region;

- It may be speculated that the rather complex tectonic structure and North Dinaric fast velocity anomaly (ND-anomaly) identified on the teleseismic tomography for the wider Kvarner region is superimposed on the lithospheric decoupling of the NW and SE fragments of the Adriatic microplate;
- The attenuation properties of rocks in the Northwestern External Dinarides are far from isotropic. The most likely anisotropy sources are the preferential orientations of cracks and fractures under the local tectonic stress field, trapping of waves along major faults (waveguides), and/or attenuation within the fault zones.

The results presented in this paper are significant for expanding knowledge on attenuation of near-surface crust layers in the similar geological and tectonical settings. Besides, the results highlight the importance of reliable information on local source model parameters. Furthermore, the use of the SAF model (Sović and Šariri, 2016) based on realistic earthquake scenarios 10 enables prediction of attenuation in specific areas.

## Acknowledgements

This work has been supported in part by Croatian Science Foundation under the projects HRZZ IP-2016-06-1854 and HRZZ IP-2014-09-9666. The authors are thankful to the University of Zagreb, Faculty of Geotechnical Engineering for the funding provided for geophysical measurements. We thank to the editor, as well as Franjo Šumanovac and one anonymous reviewer 15 for the constructive criticism on the submitted version of the manuscript.

## References

Abercrombie, R.E.: A Summary of Attenuation Measurements from Borehole Recordings of Earthquakes: The 10 Hz Transition Problem, *Pure and Applied Geophysics*, 153, 475-487, 1998.

20 Aljinović, B. and Blašković, I.: About the deep seismic horizon in the NE Adriatic area, *ZSN JAZU, Proceedings, Ser. A8*, 1, 363-380, 1981.

Aljinović, B., Blašković, I., Cvijanović, D., Prelogović, E., Skoko, D. and Brdarević, N.: Correlation of geophysical and seismological data in the coastal part of Yugoslavia, *Bulletino di Oceanologia Teorica ed Applicata*, Vol. II, N. 2, 77-90, 1984.

25 Anderson, J.G. and Hough, S.E.: A model for the shape of the Fourier amplitude spectrum of acceleration at high frequencies, *Bulletin of the Seismological Society of America*, 74, 1969-1993, 1984.

Barton, N.: Rock Quality, Seismic Velocity, Attenuation and Anisotropy, Taylor & Francis Group, London, UK/Balkema, Leiden, Netherlands, 2006.

30 Battaglia, M., Murray, M.H., Serpelloni, E. and Bürgmann, R.: The Adriatic region: An independent microplate within the Africa-Eurasia collision zone, *Geophysical Research Letters*, 31, 1-4, doi: 10.1029/2004GL019723, 2004.

Belinić, T., Stipčević, J., Živčić, M. and AlpArrayWorking Group: Lithospheric thickness under the Dinarides, *Earth and Planetary Science Letters*, 484, 229-240, doi: 10.1016/j.epsl.2017.12.030, 2018.

Beresnev, I. A., Wen, K. L.: Nonlinear soil response – a reality? *Bull. Seismol. Soc. Am.*, 86/6, 1964-1978, 1996.

Besana, G. M., Negishi, H. and Ando, M.: The three-dimensional attenuation structures beneath the Philippine archipelago based on seismic intensity data inversion, *Earth and Planetary Science Letters*, 151, 1-11, 1997.

35 Biro, Y. and Renault, P.: Importance and impact of host-to-target conversions for ground motion prediction equations in PSHA, in 15th World Conference on Earthquake Engineering, Lisbon, Portugal, 24-28 September 2012, 2012.

Boore, D.M.: Stochastic simulation of high-frequency ground motions based on seismological models of the radiated spectra, *Bulletin of the Seismological Society of America*, 73, 1865-1894, 1983.

Boore, D.M. and Joyner, W.B.: Site amplifications for generic rock sites, *Bulletin of the Seismological Society of America*, 87, 327–341, 1997.

Boore, D.M.: Simulation of Ground Motion Using the Stochastic Method, *Pure and Applied Geophysics*, 160, 635–676, doi:10.1007/PL00012553, 2003.

5 Bottari, A., Federico, B. and Lo Giudice, E.: The correlation between the macroseismic attenuation trend and the geo-structural framework; The Calabro-peloritan Arc an example, *Tectonophysics*, 108, 33-49, 1984.

Brdarević, N. and Oluić, M.: Contribution to the knowledge of tectonical structure of the Adriatic sea bottom, Rudarsko-geološko-naftni fakultet, Sveučilište u Zagrebu, *Proceedings*, 318-332, 1979.

10 Brückl, E., Bleibinhaus, F., Gosar, A., Grad, M., Guterch, A., Hrubcová, P., Keller, G.R., Šumanovac, F., Tiira, T., Yliniemi, J., Hegedűs, E., Thybo, H., 2007. Crustal structure due to collisional and escape tectonics in the Eastern Alps region based on profiles Alp01 and Alp02 from the ALP 2002 seismic experiment, *J. Geophys. Res.*, 112, B06308, doi: 10.1029/2006JB004687, 2007.

Buech, F., Davies, T. R. and Pettinga, J. R.: The Little Red Hill seismic experimental study: Topographic effects on ground motion at a bedrock-dominated mountain edifice, *Bull. Seismol. Soc. Am.*, 100/5A, 2219-2229, 2010.

15 Campbell, K. W.: Prediction of strong ground motion using the hybrid empirical method and its use in the development of ground motion (attenuation) relations in eastern North America, *Bull. Seismol. Soc. Am.*, 93, 1012–1033, 2003.

Chandler, A.M., Lam, N.T.K., Tsang, H.H. and Sheikh, M.N.: Estimation of near-surface attenuation in bedrock for analysis of intraplate seismic hazard, *Journal of Seismology and Earthquake Engineering*, 7, 159–173, 2005.

20 Dasović, I., Herak, M. and Herak, D.: Attenuation of coda waves in the contact zone between the Dinarides and the Adriatic Microplate, *Studia Geophysica et Geodaetica*, 56, 231–247, doi:10.1007/s11200-010-0077-8, 2012.

Dasović, I., Herak, M. and Herak, D.: Coda-Q and its lapse time dependence analysis in the interaction zone of the Dinarides, the Alps and the Pannonian basin, *Physics and Chemistry of the Earth*, 63, 47–54, doi:10.1016/j.pce.2013.03.001, 2013.

25 Dasović, I.: Attenuation of seismic waves beneath the Dinarides. (Ph.D. dissertation), University of Zagreb, Faculty of Science, Zagreb, Croatia, p125., 2015.

Delavaud, E., Cotton, F., Akkar, S., Scherbaum, F., Danciu, L., Beauval, C., Drouet, S., Douglas, J., Basili, R., Sandikkaya, M.A., Segou, M., Faccioli, E. and Theodoulidis, N.: Toward a ground-motion logic tree for probabilistic seismic hazard assessment in Europe, *Journal of Seismology*, 16, 451–473, doi:10.1007/s10950-012-9281-z, 2012.

30 Del Monaco, F., Tallini, M., De Rose, C. and Durante, F.: HVNSR survey in historical downtown L’Aquila (central Italy): Site resonance properties vs. subsoil model, *Engineering Geology*, 158, 34–47, doi:10.1016/j.enggeo.2013.03.008, 2013.

Di Giacomo, D., Gallipoli, M.R., Mucciarelli, M., Parolai, S. and Richwalski, S.M.: Analysis and modeling of HVSR in the presence of a velocity inversion: The case of Venosa, Italy, *Bulletin of the Seismological Society of America*, 95, 2364–2372, doi:10.1785/0120040242, 2005.

35 Drouet, S., Cotton, F. and Guéguen, P.: VS30,  $\kappa$ , regional attenuation and Mw from accelerograms: Application to magnitude 3-5 French earthquakes, *Geophysical Journal International* 182, 880–898, doi:10.1111/j.1365-246X.2010.04626.x, 2010.

40 Durasek, N., Frank, G., Jenko, K., Kužina, A. and Tončić-Gregl, R.: Prilog poznavanju naftno-geoloških odnosa u sjeverozapadnom dijelu jadranskog podmorja (Contribution to the understanding of oil-geological relations in NW Adriatic area). In: A. Šolc (Editor), *Kompleksna naftno-geološka problematika podmorja i priobalnih dijelova Jadranskog mora (Complex Oil-geological Aspects for Offshore and Coastal Adriatic Areas)*, Split, *Zbornik radova (Proceedings)* I, pp. 201-213, 1981.

Edwards, B., Fäh, D. and Giardini, D.: Attenuation of seismic shear wave energy in Switzerland, *Geophysical Journal International*, 185, 967–984, doi:10.1111/j.1365-246X.2011.04987.x, 2011.

45 Finetti, I.R., Ed.: Depth contour Map of the Moho discontinuity in the Central Mediterranean region from new CROP seismic data, In: Finetti, I. R. (Ed.), *CROP Project, Deep Seismic Exploration of the Central Mediterranean and Italy, Atlases in Geoscience*, 1, 597-606, and Chapter 27, Plate 1 (map), Elsevier, New York, 2005.

Geli, L., Bard, P. Y., and Jullien, B.: The effect of topography on earthquake ground motion: A review and new results, *Bull. Seismol. Soc. Am.*, 81/1, 42-63, 1988.

Grad, M., Tiira, T., and ESC Working Group: The Moho depth map of the European Plate, *Geophys. J. Int.* 176, 279–292, doi: 10.1111/j.1365-246X.2008.03919.x, 2009.

Gentili, S. and Franceschina, G.: High frequency attenuation of shear waves in the southeastern Alps and northern Dinarides, *Geophysical Journal International*, 185, 1393–1416, doi:10.1111/j.1365-246X.2011.05016.x, 2011.

5 Gosar, A.: Microtremor HVSR study for assessing site effects in the Bovec basin (NW Slovenia) related to 1998 Mw5.6 and 2004 Mw5.2 earthquakes, *Engineering Geology*, 91, 178–193, doi:10.1016/j.enggeo.2007.01.008, 2007.

Gosar, A. and Martinec, M.: Microtremor HVSR study of site effects in the Ilirska Bistrica town area (S.Slovenia), *Journal of Earthquake Engineering*, 30, 13-50, doi:10.1080/13632460802212956, 2009.

10 Gosar, A., Rošer, J., Šket-Mošnikar, B. and Zupančić, P.: Microtremor study of site effects and soil-structure resonance in the city of Ljubljana (central Slovenia), *Bulletin of Earthquake Engineering*, 8, 571–592, doi:10.1007/s10518-009-9113-x, 2010.

Grandić, S., Biancone, M. and Samaržija, J.: Geophysical and Stratigraphic Evidence of the Adriatic Triassic Rift Structures, *Mem. Soc. Geol. It.*, 57, 315–325, 2002.

15 Gravity map of Yugoslavia, *Gravimetrijska karta SFR Jugoslavije - Bouguerove anomalije*, 1:500.000, Federal Geological Institute, Beograd, 1972.

Handy, M. R., Ustaszewski, K. and Kissling, E.: Reconstructing the Alps-Carpathians-Dinarides as a key to understanding switches in the subduction polarity, slab gaps and surface motion, *Int. J. Earth Sci. (Geol Rundsch)*, 104, 1–26, doi:10.1007/s00531-014-1060-3, 2015.

20 Hanks, T.C. and McGuire, R.K.: The character of high-frequency strong ground motion, *Bulletin of the Seismological Society of America*, 71, 2071–2095, 1981.

Hashida, T., Stavrakakis, G. and Shimazaki, K.: Three-dimensional seismic attenuation structure beneath the Aegean region and its tectonic implication, *Tectonophysics*, 145, 43-54, 1988.

Herak, M., Herak, D. and Markušić, S.: Revision of the earthquake catalogue and seismicity of Croatia, 1908–1992, *Terra Nova*, 8, 86–94, 1996.

25 Herak, M., Allegretti, I., Herak, D., Kuk, K., Kuk, V., Marić, K., Markušić, S. and Stipčević, J.: HVSR of ambient noise in Ston (Croatia): Comparison with theoretical spectra and with the damage distribution after the 1996 Ston-Slano earthquake, *Bulletin of Earthquake Engineering*, 8, 483–499, doi:10.1007/s10518-009-9121-x, 2010.

Herak, M.: Overview of recent ambient noise measurements in Croatia in free-field and in buildings, *Geofizika*, 28, 21-40, 2011.

30 HGI: Geološka karta Republike Hrvatske mjerila 1:300.000 (Geological Map of the Republic of Croatia, scale 1:300.000), Hrvatski geološki institut – Croatian Geological Survey, <http://webgis.hgi-cgs.hr/gk300/default.aspx>, 2009.

Ivančić, I., Herak, D., Markušić, S., Sović, I. and Herak, M.: Seismicity of Croatia in the period 2002–2005, *Geofizika*, 23, 87–103, 2006.

35 Ivančić, I., Herak, D., Herak, M., Allegretti, I., Fiket, T., Kuk, K., Markušić, S., Prevolnik, S., Sović, I., Dasović, I. and Stipčević, J.: Seismicity of Croatia in the period 2006–2015, *Geofizika*, 35, 69-98, doi: 10.15233/gfz.2018.35.2, 2018.

Johnson, P. A. and Jia, X.: Nonlinear dynamics, granular media and dynamic earthquake triggering, *Nature*, 437/6, 871–874, doi:10.1038/nature04015, 2005.

Johnston, D.H., Toksöz, M.N. and Timur, A.: Attenuation of seismic waves in dry and saturated rocks: II. Mechanisms, *Geophysics*, 44(4), 691–711, 1979.

40 Korbar, T.: Orogenic evolution of the External Dinarides in the NE Adriatic region: a model constrained by tectonostratigraphy of Upper Cretaceous to Paleogene carbonates, *Earth Sci. Rev.*, 96, 296–312, 2009.

Kövesligethy von, R.: Seismischer Stärkegrad und Intensität der Beben, *Gerlands Beiträge zur Geophysik*, Band VIII, Leipzig, 1907.

Ktenidou, O.J., Gélis, C. and Bonilla, L.F.: A study on the variability of Kappa ( $\kappa$ ) in a Borehole: Implications of the computation process, *Bulletin of the Seismological Society of America*, 103, 1048–1068, doi:10.1785/0120120093, 2013.

45 Ktenidou, O.-J., Cotton, F., Abrahamson, N.A. and Anderson, J.G.: Taxonomy of  $\kappa$ : a review of definitions and estimation approaches targeted to applications, *Seismological Research Letters*, 85, 135–146, doi:10.1785/0220130027, 2014.

Ktenidou, O.J., Abrahamson, N.A., Drouet, S. and Cotton, F.: Understanding the physics of kappa ( $\kappa$ ): Insights from a 50 downhole array, *Geophysical Journal International*, 203, 678–691, doi:10.1093/gji/ggv315, 2015.

Kuk, V., Prelogović, E. and Dragičević, I.: Seismotectonically active zones in the Dinarides, *Geol. Croat.*, 53(2), 295-303, 2000.

Lekkas, E.: The Athenas earthquake (7 September 1999); intensity distribution and controlling factors, *Engineering Geology*, 59, 297-311, 2001.

5 Mucciarelli, M. and Gallipoli M.R.: A critical review of 10 years of microtremor HVSR technique, *Bolletino di Geofisica Teorica ed Applicata*, 42/3-4, 255-266, 2001.

Oldow, J.S., Ferranti, L., Lewis, D.S., Campbell, J.K., D'Argenio, B., Catalano, R., Pappone, G., Carmignani, L., Conti, P. and Aiken, C.L.V.: Active fragmentation of Adria, the north African promontory, central Mediterranean region, *Geology*, 30/9, 779-782, 2002.

10 Orešković, J., Šumanovac, F., Hegedűs, E.: Crustal structure beneath Istra peninsula based on receiver function analysis, *Geofizika*, 28, 247-263, 2011.

Panzera, F., Lombardo, G., D'Amico, S. and Galea, P.: Speedy Techniques to Evaluate Seismic Site Effects in Particular Geomorphologic Conditions: Faults, Cavities, Landslides and Topographic Irregularities (Chapter 5), InTech, 102-138, 2013.

15 Perron, V., Hollender, F., Bard, P.Y., Gélis, C., Guyonnet-Benaize, C., Hernandez, B. and Ktenidou, O.J. Robustness of kappa ( $\kappa$ ) measurement in low-to-moderate seismicity areas: Insight from a site-specific study in provence, France, *Bulletin of the Seismological Society of America*, 107, 2272-2292, doi:10.1785/0120160374, 2017.

Placer, L., Vrabec, M. and Celarc, B.: The bases for understanding of the NW Dinarides and Istria Peninsula tectonics, *Geologija*, 53/1, 55-86, 2010.

20 Prelogović, E., Cvijanović, D., Aljinović, B., Kranjec, V., Skoko, D., Blašković, I. and Zagorac, Ž.: Seizmotektonika aktivnost duž priobalnog dijela Jugoslavije (in Croatian), *Geološki vjesnik*, 35, 195-207, 1982.

Reiter, L.: Earthquake Hazard Analysis: Issues and insights, Columbia University Press, p.254, 1990.

Schmid, S.M., Bernoulli, D., Fügenschuh, B., Matenco, L., Schefer, S., Schuster, R., Tischler, M. and Ustaszewski, K.: The Alps-Carpathians-Dinarides-connection: a correlation of tectonic units, *Swiss J. Geosci.*, 101, 139-183, 2008.

25 Seed, H. B. and Schnabel, P. B.: Soil and Geological Effects on Site Response During Earthquakes, *Proc. of First International Conf. on Microzonation for Safer Construction – Research and Application*, vol. I, 61-74, 1972.

Sović, I., Šariri, K. and Živčić, M.: High frequency microseismic noise as possible earthquake precursor, *Research in Geophysics*, 3, 1, doi: 104081/rge.2013. e2, 2013.

30 Sović, I. and Šariri, K.: Explaining anisotropic macroseismic fields in terms of fault zone attenuation - a simple model, *Tectonophysics*, 680, 113-121 doi:10.1016/j.tecto.2016.05.018, 2016.

Sović, I., Šariri, K. and Tasić, T.: Image processing in macroseismology: use of the image moments analysis for the comparison of isoseismal maps // 35th General Assembly of the ESC - Book of Abstracts / Marco Mucciarelli (ed.). Trieste : ESC - OGS, 395, 2016.

35 Sović, I. and Šariri, K.: A simple anisotropic model of macroseismic field, 36th General Assembly of the ESC - Book of Abstracts, Valletta, Malta, 2018.

Stanko, D., Markušić, S., Strelec, S. and Gazdek, M.: Seismic response and vulnerability of historical Trakošćan Castle using HVSR method, *Environ Earth Sci.*, 75, 368, doi:10.1007/s12665-015-5185-x, 2016.

40 Stanko, D., Markušić, S., Strelec, S. and Gazdek, M.: HVSR analysis of seismic site effects and soil-structure resonance in Varaždin city (North Croatia), *Soil Dynamics and Earthquake Engineering*, 92, 666-677, doi:10.1016/j.soildyn.2016.10.022, 2017.

Šumanovac, F.: Lithosphere structure at the contact of the Adriatic microplate and the Pannonian segment based on the gravity modelling, *Tectonophysics*, 485, 94-106, doi:10.1016/j.tecto.2009.12.005, 2010.

45 Šumanovac, F., Orešković, J., Grad, M., ALP2002 Working Group: Crustal structure at the contact of the Dinarides and Pannonian basin based on 2-D seismic and gravity interpretation of the Alp07 profile in the ALP2002 experiment, *Geophys. J. Int.*, 179, 615-633, doi:10.1111/j.1365-246X.2009.04288.x, 2009.

Šumanovac, F. and Dudjak, D.: Descending lithosphere slab beneath the Northwest Dinarides from teleseismic tomography, *Journal of Geodynamics*, 102, 171-184, doi:10.1016/j.jog.2016.09.007, 2016.

50 Šumanovac, F., Markušić, S., Engelsfeld, T., Jurković, K. and Orešković, J.: Shallow and deep lithosphere slabs beneath the Dinarides from teleseismic tomography as the result of the Adriatic lithosphere downwelling, *Tectonophysics*, 712-713, 523-541, doi: 10.1016/j.tecto.2017.06.018, 2017.

Tomljenović, B., Csontos, L., Marton, E. and Marton, P.: Tectonic evolution of the northwestern Internal Dinarides as constrained by structures and rotation of Medvednica Mountains, North Croatia, Geological Society, London, Special Publications, 298, 145–167, doi:10.1144/SP298.8, 2008.

Van Houtte, C., Drouet, S. and Cotton, F.: Analysis of the origins of  $\kappa$  (kappa) to compute hard rock to rock adjustment factors for GMPEs, Bulletin of the Seismological Society of America, 101, 2926–2941, doi:10.1785/0120100345, 2011.

5 Velić, I and Vlahović, I. (eds): Explanatory notes for the Geological Map of the Republic of Croatia, scale 1:300000, Croatian Geological Survey. p. 147, 2009.

Vlahović, I., Tišljar, J., Velić, I. and Matičec, D.: Evolution of the Adriatic Carbonate Platform: palaeogeography, main events and depositional dynamics, Palaeogeography, Palaeoclimatology, Palaeoecology, 220/3–4, 333–360, 2005.

10 Worthington, M.H. and Hudson, J.A.: Fault properties from seismic Q, Geophysical Journal International, 143(3), 937–944, 2000.

York, D., Evenson, N., Martinez, M. and Delgado, J.: Unified equations for the slope, intercept, and standard errors of the best straight line, American Journal of Physics, 72, 367–375, 2004.

## Tables and Figures

**Table 1: Number of analyzed earthquakes, and  $V_{S30}$  for each station.**

5 \*Approximated as soil category A from EC8 due to the problem to obtain permit for geophysical survey in the Brijuni National Park (BRJN station).

| Station | Time period | Number of EQs | $V_{S30}$ (m/s) |
|---------|-------------|---------------|-----------------|
| BRJN    | 2009–2013   | 33            | *EC8-A          |
| RIY     | 2006–2016   | 60            | $\approx 1190$  |
| NVLJ    | 2002–2016   | 107           | $\approx 1270$  |
| OZLJ    | 2011–2016   | 35            | $\approx 850$   |

10

**Table 2: Summarized results of errors-in-variables regression (following the method by York et al. 2004) for  $\kappa - R_e$  dependence based on horizontal and vertical component  $\kappa$  models ( $\kappa_{hor}$  and  $\kappa_{ver}$ ) using the AH84 model. Site-specific (near-site) attenuation values  $\kappa_0^{hor}$  and  $\kappa_0^{ver}$ , slopes of regression in terms of  $\kappa_R^{hor}$  and  $\kappa_R^{ver}$ , standard errors SE for intercepts and slopes and ratios of  $\kappa_0^{ver}/\kappa_0^{hor}$  and  $\kappa_R^{ver}/\kappa_R^{hor}$  are listed for each seismological station. Standard errors (SE) for the intercept and slope are also listed.**

15

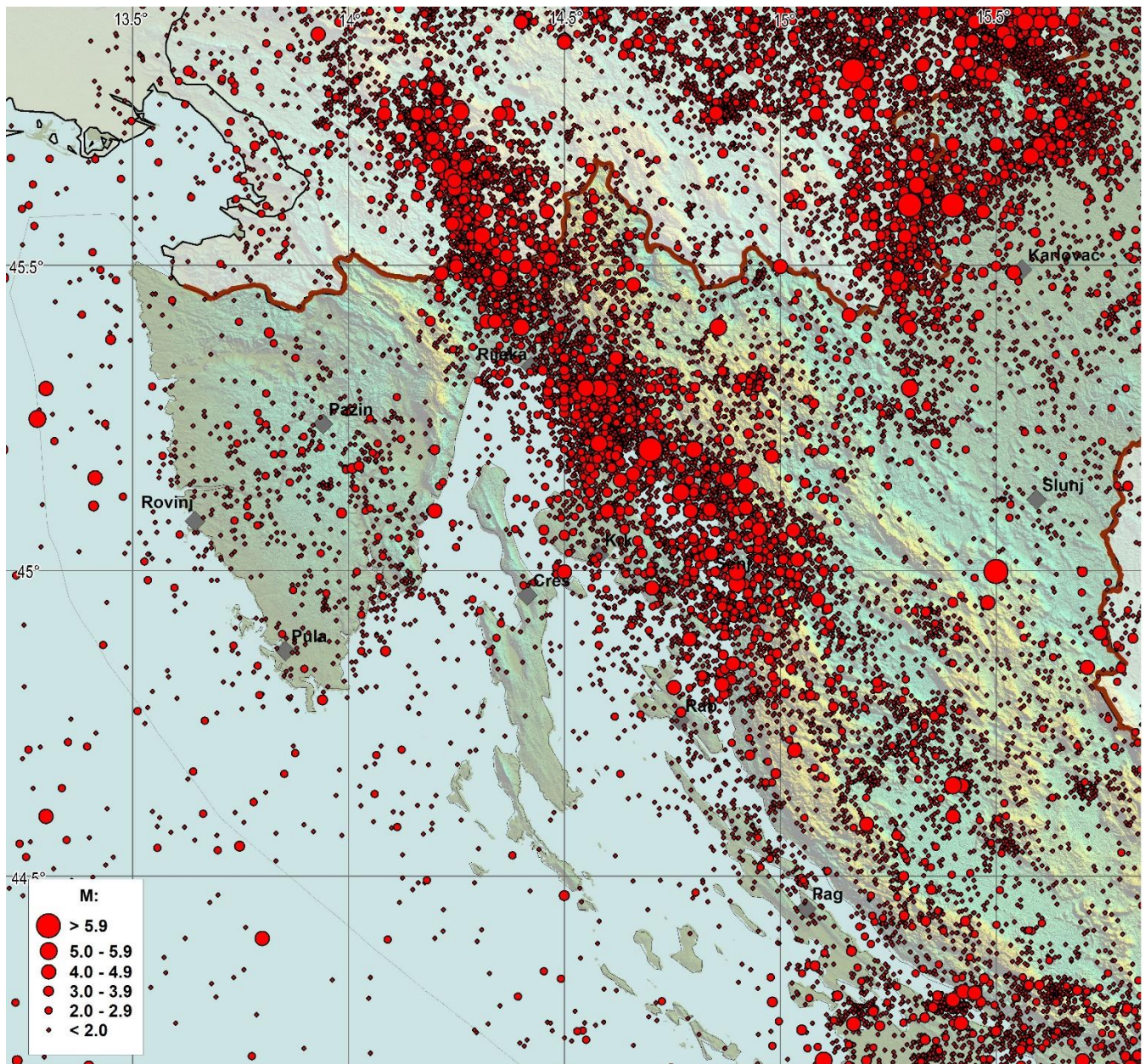
|   | BRJN            | RIY             | NVLJ            | OZLJ            |
|---|-----------------|-----------------|-----------------|-----------------|
| $\kappa_0^{hor}$ (s)                      | <b>0.0249</b>   | <b>0.0239</b>   | <b>0.0235</b>   | <b>0.0377</b>   |
| SE- $\kappa_0^{hor}$ (s)                  | 0.0045          | 0.0024          | 0.0020          | 0.0024          |
| $\kappa_R^{hor}$ (skm <sup>-1</sup> )     | <b>0.000131</b> | <b>0.000196</b> | <b>0.000172</b> | <b>0.000237</b> |
| SE- $\kappa_R^{hor}$ (skm <sup>-1</sup> ) | 0.000039        | 0.000025        | 0.000019        | 0.000042        |
| $\kappa_0^{ver}$ (s)                      | <b>0.0362</b>   | <b>0.0212</b>   | <b>0.0225</b>   | <b>0.0412</b>   |
| SE- $\kappa_0^{ver}$ (s)                  | 0.0054          | 0.0031          | 0.0027          | 0.0040          |
| $\kappa_R^{ver}$ (skm <sup>-1</sup> )     | <b>0.000110</b> | <b>0.000219</b> | <b>0.000152</b> | <b>0.000204</b> |
| SE- $\kappa_R^{ver}$ (skm <sup>-1</sup> ) | 0.000047        | 0.000032        | 0.000026        | 0.000043        |
| $\kappa_0^{ver}/\kappa_0^{hor}$           | 1.45            | 0.89            | 0.96            | 1.09            |
| $\kappa_R^{ver}/\kappa_R^{hor}$           | 0.84            | 1.11            | 0.88            | 0.87            |

Table 3: Values of  $Q_0^C$  and  $n_c$  for the lapse time of the coda waves window  $t_L = 30$  s (Dasović 2015 – most recent values),  $Q_{est}^C$  estimated for the high frequency range (10–25 Hz) from  $Q_{est}^C(f) = Q_0^C f c^n$  and frequency-independent  $Q_{est}(K_R)$ .  
5 There is no published information for the BRJN station regarding the existence of the frequency dependent ( $f$ ).

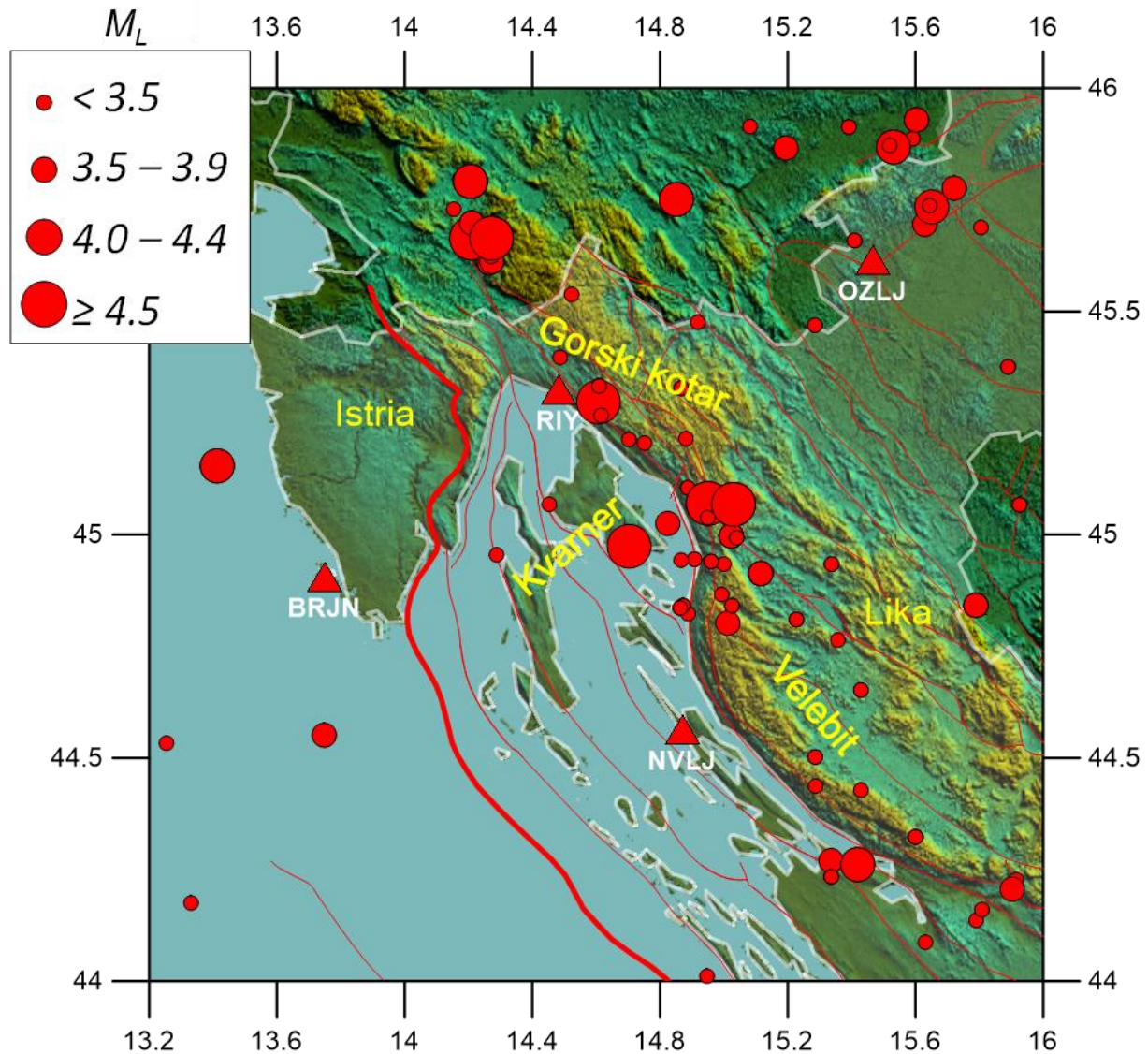
| Station | $Q_0^C$ | $n_c$ | $Q_{est}^C$<br>(10-25 Hz) | $K_R$ (skm $^{-1}$ ) | $Q_{est}(K_R)$ |
|---------|---------|-------|---------------------------|----------------------|----------------|
| BRJN    | -       | -     | -                         | 0.000131             | 2181           |
| RIY     | 84      | 0.93  | 715-1362                  | 0.000196             | 1458           |
| NVLJ    | 89      | 1.16  | 1286-2875                 | 0.000172             | 1661           |
| OZLJ    | 78      | 0.69  | 382-616                   | 0.000237             | 1206           |

10 Table 4: Basic parameters for the set of earthquakes that were macroseismically investigated.

| Date<br>(yyyy/mm/dd) | Time<br>(GMT) | Latitude<br>(°N) | Longitude<br>(°E) | $I_o$<br>°MSK | $I_{max}$<br>°MSK | $M_L$ |
|----------------------|---------------|------------------|-------------------|---------------|-------------------|-------|
| 1870/03/01           | 19:57         | 45.510           | 14.332            |               | VIII              |       |
| 1916/03/12           | 03:23         | 45.140           | 14.920            | VIII          |                   | 5.8   |
| 1939/02/05           | 22:00         | 45.150           | 14.630            | VI-VII        |                   | 4.6   |
| 1939/02/06           | 07:23         | 45.160           | 14.660            | VI-VII        |                   | 4.9   |
| 2007/02/05           | 08:30         | 45.070           | 14.950            |               | VII               | 4.9   |
| 2013/07/30           | 12:58         | 45.068           | 15.030            |               | VI                | 4.8   |



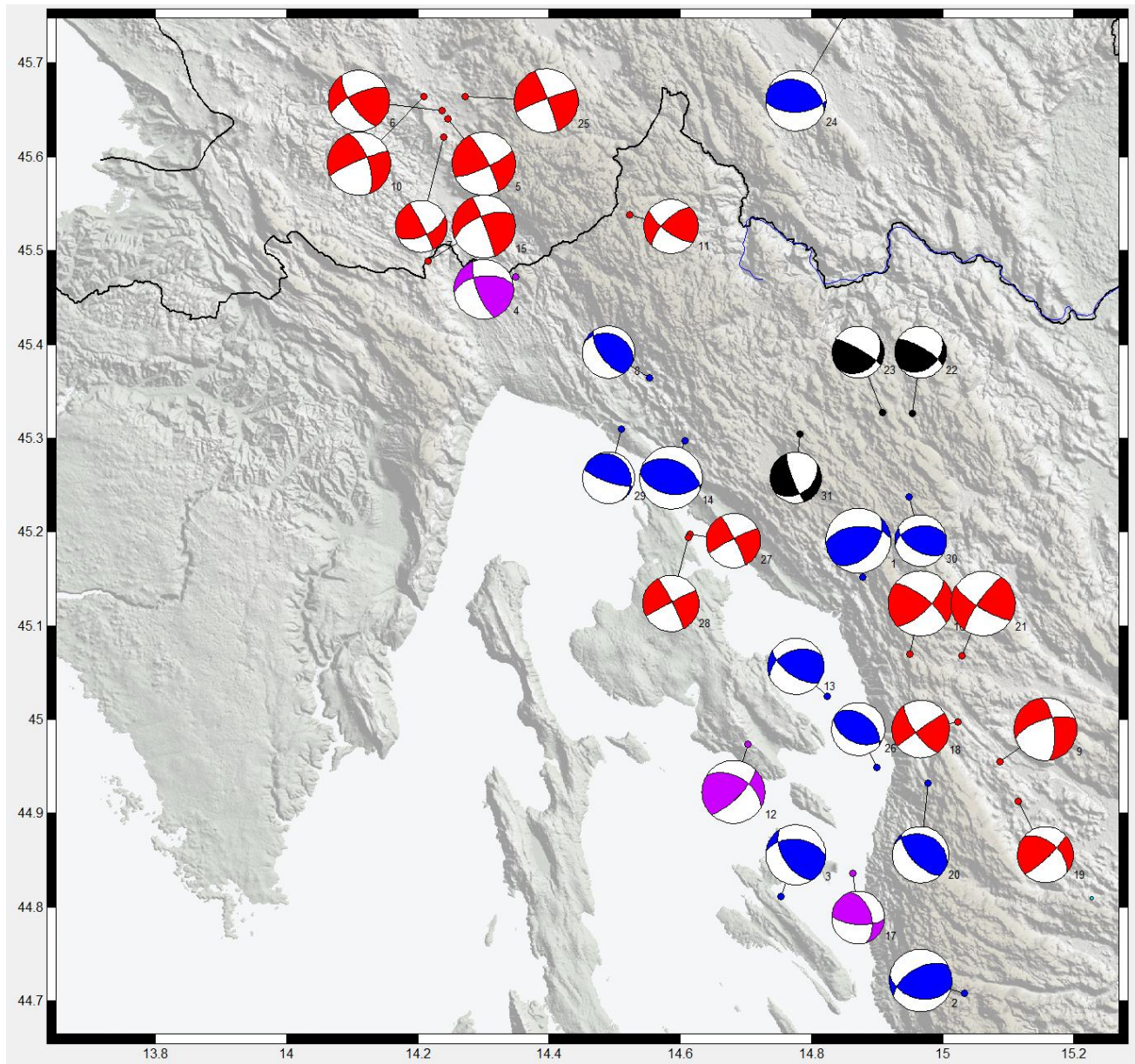
**Figure 1: Spatial distribution of earthquake locations in the investigated area (373BC – 2017, according to the Croatian Earthquake Catalog - CEC, updated version first described in Herak et al., 1996).**



5

**Figure 2: Topographic map of the study area with earthquake epicenters (2002–2016) used for kappa calculation. Red triangles mark the locations of seismic stations. Red lines represent possible seismogenic surface faults in Croatia (Ivančić et al., 2006). The thick red line designates frontal Dinaridic structures as well as the boundary between the External Dinarides and the Adriatic foreland.**

10



5 **Figure 3: Focal mechanisms for regional earthquakes ( $M_w \geq 3.0$ ) from the Croatian source mechanism database. Stereographic projection of the lower focal hemisphere was used. Compressional area is marked in blue for predominantly reverse faulting, red for the strike-slip faulting while the black colour indicates sources were the faulting style could not be determined.** 

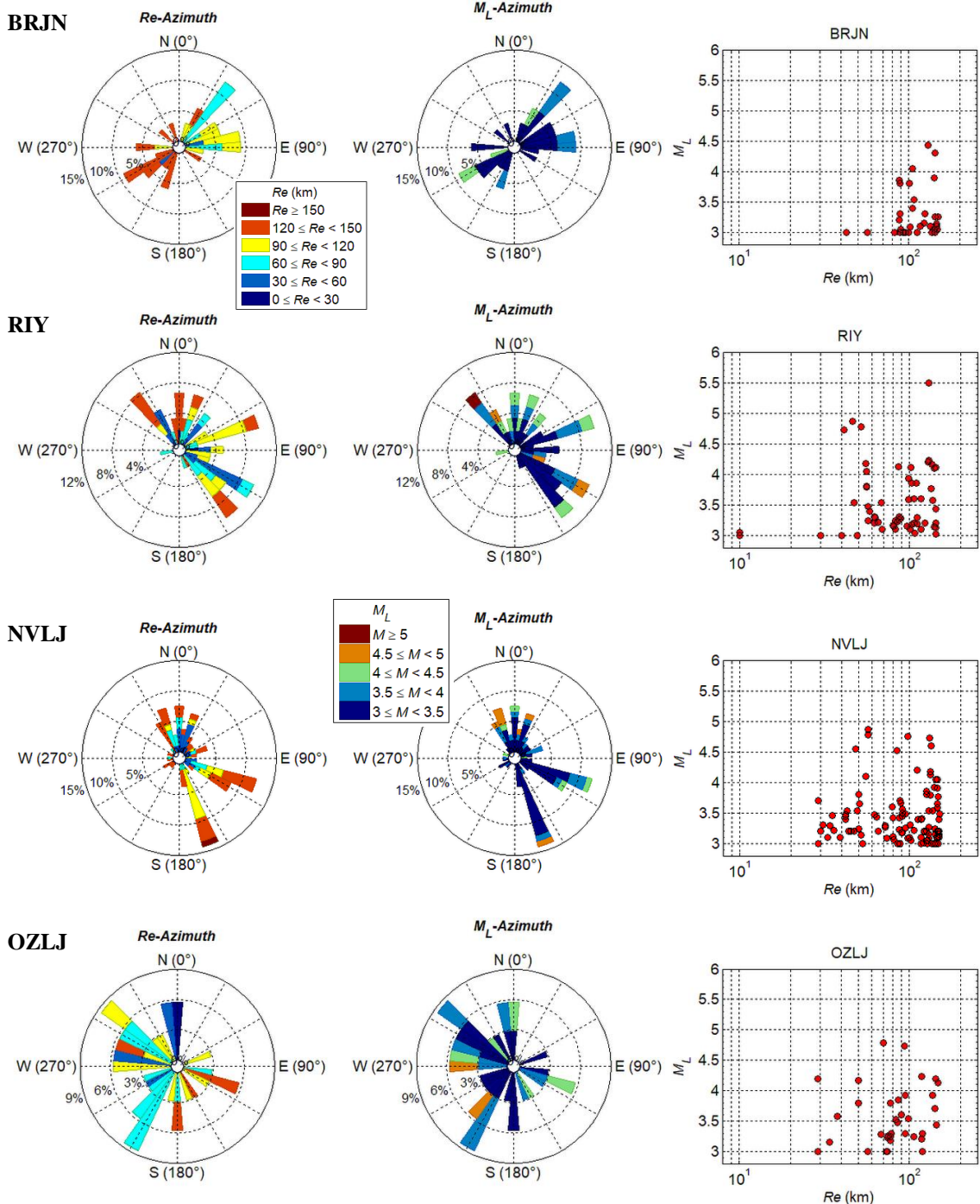
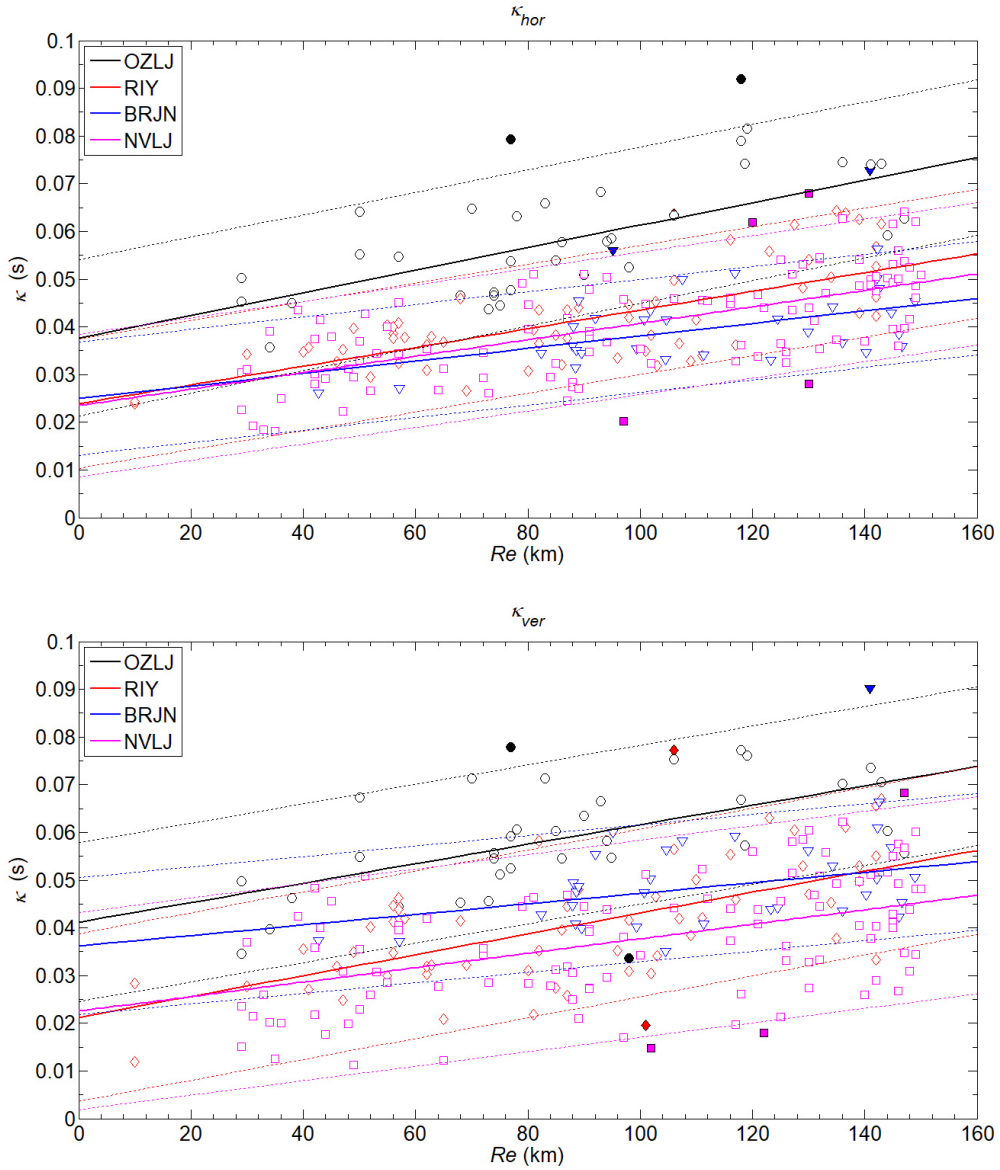


**Figure 4: Statistics of the compiled ground motion dataset. Left: azimuthal distribution of  $R_e$ . Middle: azimuthal distribution of  $M_L$ . Right:  $R_e - M_L$  distribution of recordings at each station.**



5

**Figure 5: Horizontal and vertical  $\kappa - R_e$  models for each seismological station. Site-specific attenuation values of  $\kappa_0^{hor,ver}$  (intercept at zero distance  $R_e$ ) and regression slopes  $\kappa_R^{hor,ver}$  are given in Table 2. Full markers are regression outliers outside of a 95% confidence interval (dashed lines).**

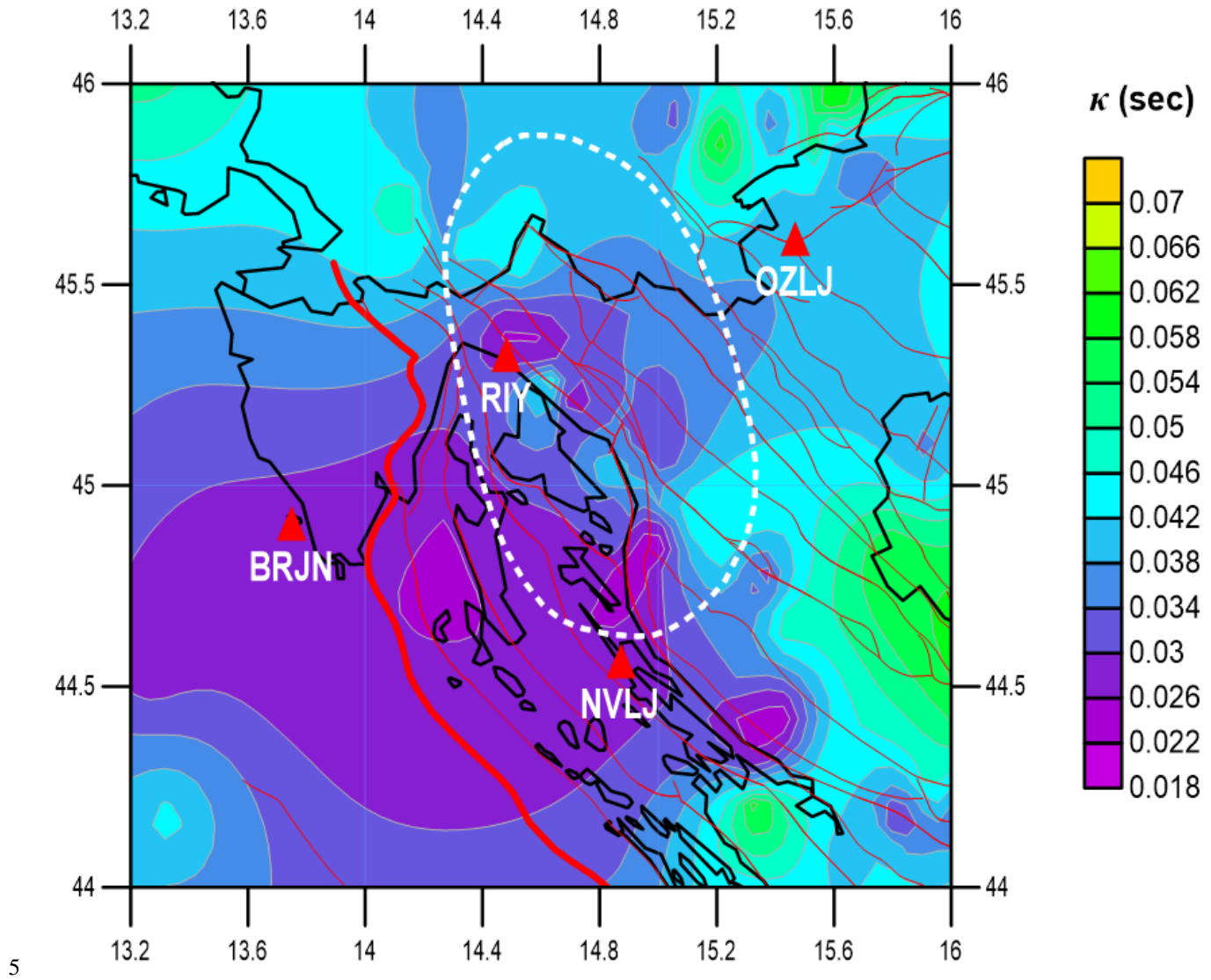
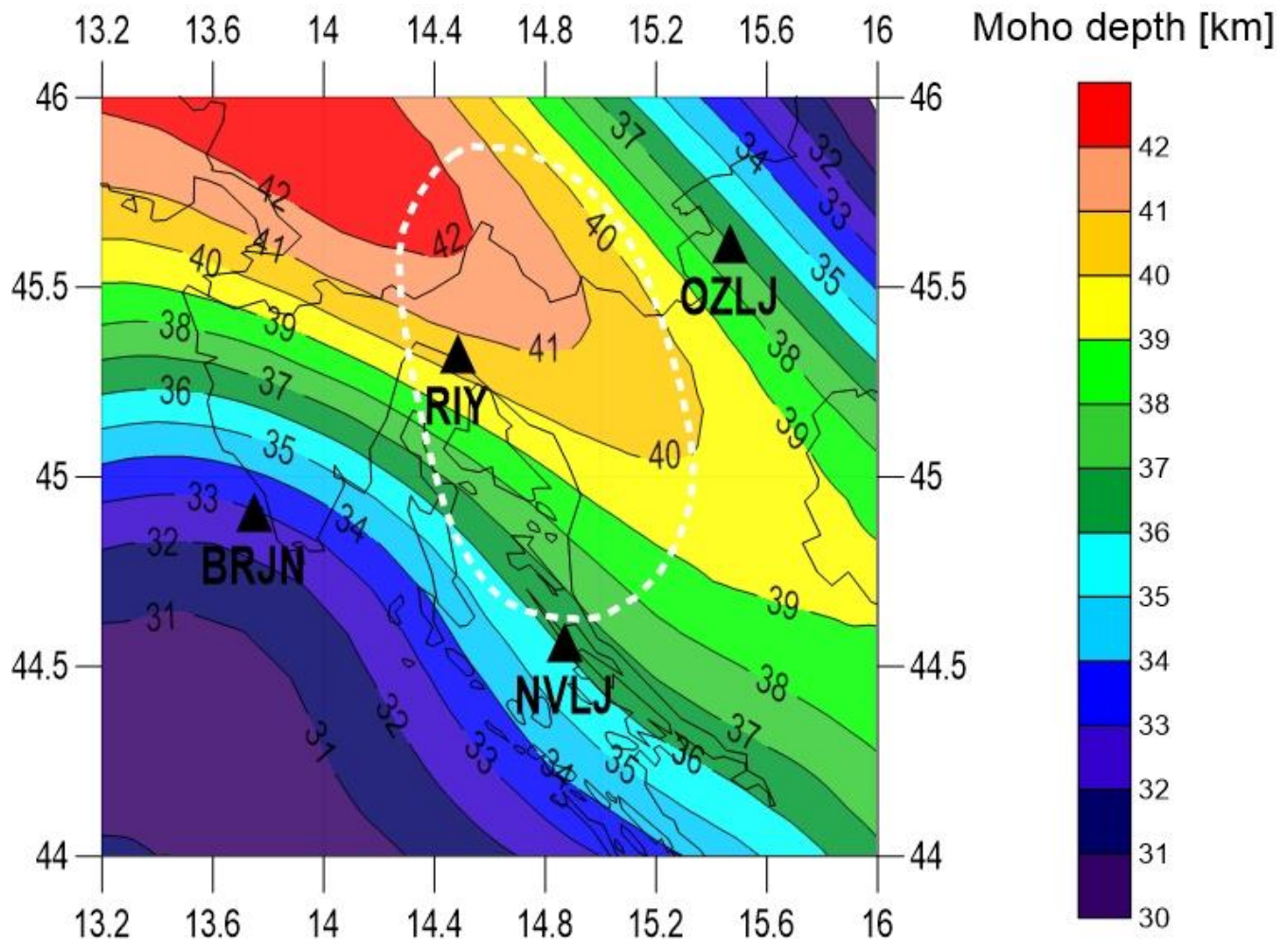


Figure 6: Regional  $\kappa$  dependence around each seismological station shown as a spatial distribution of individual  $\kappa$  values and plotted using the nearest-neighbour interpolation method. The red lines represent the possible seismogenic surface faults in Croatia as well as Bosnia and Herzegovina (Ivančić et al., 2006). The locations of the seismic stations are marked with red triangles. A thick white dashed line marks the contours of the North Dinaric (ND) fast velocity anomaly (Šumanovac and Dudjak, 2016). The thick red line marks the frontal Dinaridic structures and the boundary between the External Dinarides and the Adriatic foreland.



5

Figure 7: The Moho depth (Grad et al., 2009) at the study area. A thick white dashed line marks the contours of the North Dinaridic fast velocity anomaly determined by the teleseismic tomography (ND-anomaly) (Šumanovac and 10 Dudjak, 2016).

15

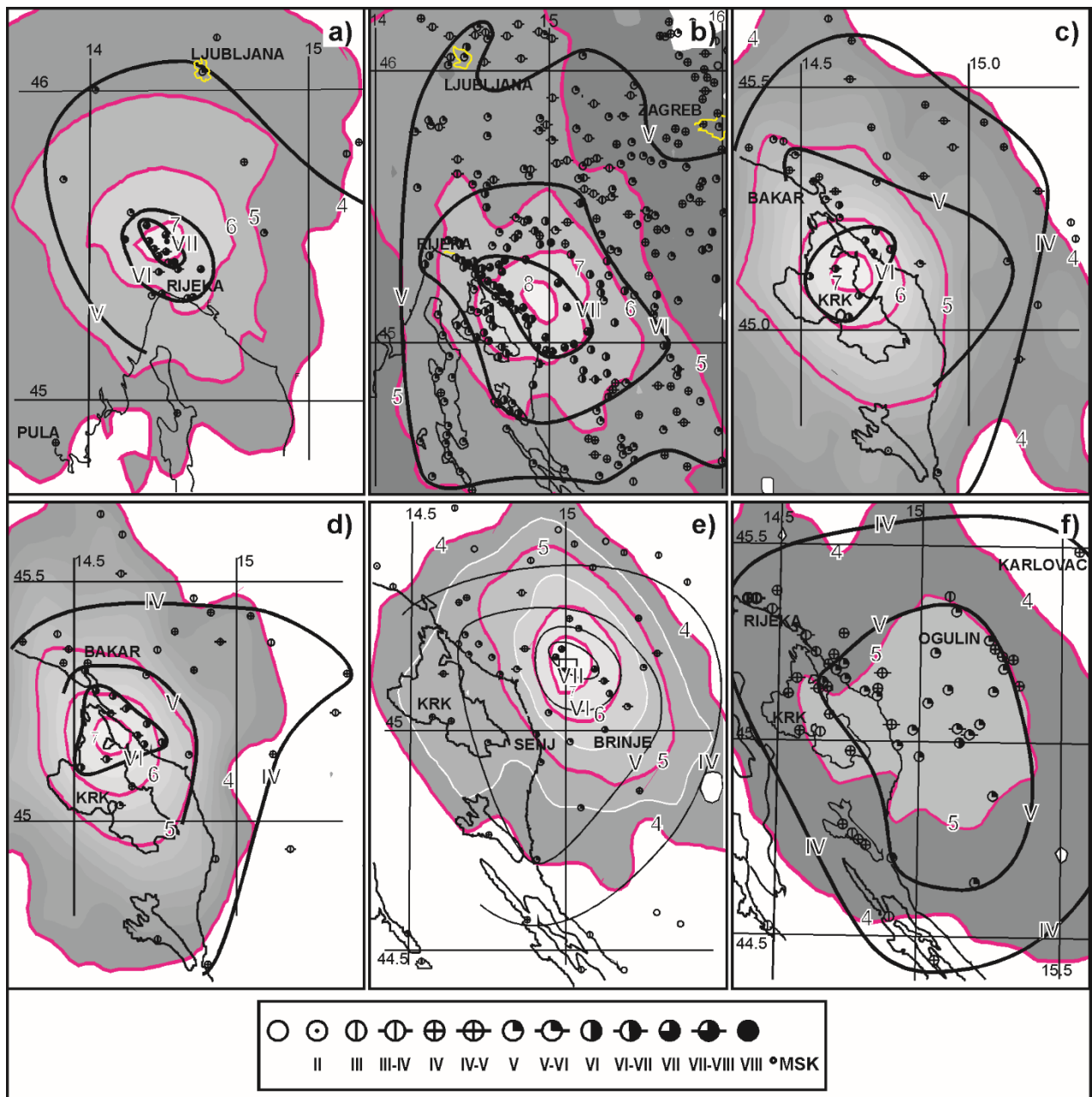


Figure 8: Empirical (black lines) and modelled (purple lines) isoseismal maps for the earthquakes (a) 1 March 1870 at 19:57 UTC; (b) 12 March 1913 at 03:23 UTC; (c) 5 February 1939 at 22:00 UTC; (d) 6 February 1939 at 07:23 UTC; (e) 5 February 2007 at 08:30 UTC; (f) 30 July 2013 at 12:58 UTC.